AIAA JOURNAL
Vol. 35, No. 11, November 1997

Analytical Study of the Oblique Reflection of Detonation Waves

H. Li* and G. Ben-Dor†
Ben-Gurion University of the Negev, Beer-Sheva 84105, Israel
and
H. Grönig‡
RWTH, Aachen D-5100, Germany

The governing equations relating the flow properties across an oblique detonation wave were reconsidered and modified by accounting for different heat capacity ratios on both side of the detonation wave. Using these equations, modified two- and three-shock-theory-based models were developed and applied to the reflection of detonation waves. The present model makes it possible to investigate the behavior of detonation wave reflections near and at the Chapman–Jouguet (CJ) point. It was shown that the properties of detonation waves near the CJ point are very sensitive to the value of the overdrive. The analytical results were compared with experimental and numerical results from various laboratories, and in general, good agreement was obtained.

Nomenclature

a	= sound speed
c_v, c_p	= specific heat capacities at constant volume and at constant pressure
h	= enthalpy
M	= Mach number of detonation or shock wave
P	= pressure
q	= heat of reaction
R	= specific gas constant
T	= temperature
U_D	= velocity of the detonation wave
u	= flow velocity
V	= specific volume
α	= overdrive
γ	= specific heat capacities ratio
θ	= flow deflection angle
θ_w, δ	= wedge angle
ρ	= density
ϕ	= angle of incidence
χ	= angle of triple point trajectory

Subscripts and Superscripts

CJ	= Chapman–Jouguet detonation
D	= detonation wave
det	= detachment point
i	= incident detonation wave
inert	= inert flow
j	= numbers of flow region, 0, 1, 2, 3
m	= Mach stem
reactive	= reactive flow
S	= shock wave
tr	= regular reflection to Mach reflection transition

Introduction

A COMPREHENSIVE review, dealing with the Mach reflection (MR) of detonation waves, which was published recently by Gelfand et al.[1] and Meltzer et al.,[2] revealed that there is still a lack of reliable analytical models by which various properties associated with the reflection of detonation waves over wedges can be accurately predicted. For example, in the case of nonreactive gases, the reflecting wedge angle at which the transition from regular reflection (RR) to MR takes place can be accurately predicted by the well-known two-shock theory of von Neumann.[3] However, in the case of reactive gases, a proposed analogous analytical model failed to predict the transition angle. Furthermore, analytical models based on the same basic ideas resulted in different results, yet unexplained. For example, using the two-shock theory, Gavrilenko et al.[4] calculated the RR ↔ MR transition angle for the mixture of $2H_2 + O_2 + 7Ar$ at 288 K and 0.2 bar to be 37 deg ± 0.4 deg, whereas Edwards et al.[5] reported two-shock theory calculations for the same mixture yielding a value of 65 deg. Note here that the experimental transition angles do not agree either. Whereas Gavrilenko and Prokhorov[6,7] reported a value of 40 deg ± 1 deg, the value reported by Edwards et al.[5] was 48 deg ± 2 deg.

Experimental and calculated results of the RR ↔ MR transition wedge angles as reported in different studies for the mixture $2H_2 + O_2 + XAr$ are summarized for the reader's convenience in Table 1. A disagreement between the experimental and analytical transition wedge angles is clearly evident in Table 1. Whereas the measured values of the RR ↔ MR transition wedge angles range from 39 to 50 deg, the values calculated using different methods range from 32 to 65 deg.

The triple point trajectory angle χ of a MR is another parameter whose analytical prediction is far from being satisfactory (e.g., see Refs. 2 and 5). For the case of nonreactive gases, this parameter is quite well predicted using the three-shock theory of von Neumann[3] together with the assumption that the Mach stem is straight and perpendicular to the reflecting surface. In reactive gases, again, not only do three-shock theory based analytical models fail to reproduce the experimental results, but also there is a large discrepancy in the literature between both experimental and calculated values.

Unlike the RR ↔ MR transition wedge angle θ_w^{tr}, which is calculated by the two-shock theory, the calculation of the triple-point trajectory angle χ is done with the three-shock theory. Consequently, the fact that the analytical predictions of both θ_w^{tr} and χ fail to agree with experimental results indicates that either the two- and the three-shock theories cannot be applied to detonation wave reflections or that the ways by which these theories have been applied to detonation wave reflections were incorrect.

As will be shown subsequently, the aforementioned discrepancies arose most likely from the fact that the analytical models of Refs. 2, 5, 6, and 8 were not good enough and from the incorrect use of a constant specific heat ratio on both sides of the detonation wave.

Based on the foregoing discussion, the objective of this study was to develop reliable analytical models for predicting various

Received Dec. 3, 1996; revision received June 27, 1997; accepted for publication July 12, 1997.

*Postdoctoral Fellow, Pearlstone Center for Aeronautical Engineering Studies, Department of Mechanical Engineering; currently Research Fellow, Center for Energy and Combustion Research, University of California, San Diego, La Jolla, CA 92093.

†Professor and Dean, Faculty of Engineering Sciences, Pearlstone Center for Aeronautical Engineering Studies, Department of Mechanical Engineering.

‡Professor, Stosswellenlabor.

Table 1 RR ↔ MR transition wedge angle for $2H_2 + O_2 + XAr \rightarrow 2H_2O + XAr$

Research group	X	Experimental result, deg	Analytical result, deg	Remark no.[a]
Edwards et al.[5]	1	46–50	65	1
Meltzer et al.[2]	0	40–45	32	——
	5	——	32	2
	7	——	32	——
Gavrilenko and Prokhorov[6]	0	39–41	34	3
	7	——	37	——
Yu and Grönig[8]	0	——	50	4
	7	——	55	4
	7	——	50–53	5

[a] 1, Modification of Whitham's theory; 2, modification of three-shock theory with constant γ; 3, not specified in the paper; 4, computational fluid dynamics with simplified chemistry; and 5, computational fluid dynamics without reaction ($\gamma = 1.58$).

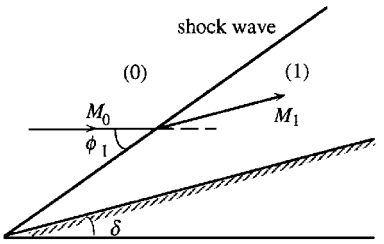

a) Inert flow with an oblique shock wave

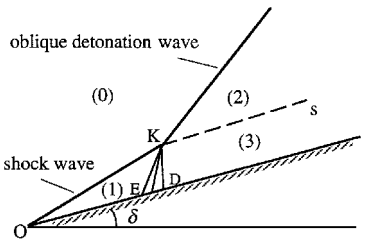

b) Reactive flow with an oblique detonation wave

Fig. 1 Schematic illustration of the flowfield that results from a supersonic flow over a sharp wedge.

parameters associated with wave configurations constructed of oblique detonation waves, while accounting for different specific ratios on both sides of the detonation waves as was originally suggested by Ref. 9.

Present Study

Because the building blocks of both the two- and the three-shock theories are the conservation equations of mass, linear momentum, tangential momentum, and energy across an oblique shock wave, it is important to check how well these equations can be used to calculate the properties of oblique detonation waves.

A numerical study of oblique detonation waves that was published recently by Li et al.[10] suggested that, unlike the case of an inert (nonreactive) gas, shown in Fig. 1a, where a straight and attached oblique shock wave emanates from the leading edge of the reflecting wedge, a different structure, shown in Fig. 1b, is obtained when the gas is reactive and the kinetic energy of the incoming flow is sufficiently less than the activation energy of the chemical reaction. The oblique shock wave has, in this case, two different parts that have distinct shock angles. In the region near the leading edge of the reflecting wedge (point O), the shock angle is identical to that appropriate to a shock in an inert gas. Behind this part of the shock, all of the fluid properties remain constant, except the induction parameter. In this region, combustion intermediates are produced so that the value of the induction parameter increases with increasing distance from the leading edge of the wedge. When the concentration of the intermediates in the flow becomes high enough to cause water formation and the associated energy release, the induction parameter becomes unity, marking the end of the induction zone. Behind the induction zone, water is produced, and a set of deflagration waves is generated near the wall. These deflagration waves represent gradual changes in the pressure and the temperature generated by the energy release in the water formation. The deflagration waves propagate upward at the local Mach angle. The Mach angle becomes steeper for each successive deflagration wave due to the increasing temperature across these waves. Therefore, they gradually converge into each other. Eventually they intersect at point K and steepen the original oblique shock wave. This steepened shock wave produces substantially higher temperatures and sharply reduces the induction delay in the flow behind this part of the shock wave. When the induction delay becomes short enough, the oblique shock wave and the initiation of energy release are closely coupled. Behind the two different parts of the shock wave structure, the density, the temperature, and the velocity after the energy release are different due to the different shock wave strengths. Therefore, a slip line separates these two regions.

The numerical results of Li et al.[10] indicated that the length of the nonreactive shock ($\overline{OK}$ in Fig. 1b) decreases as the reflecting wedge angle δ increases for a constant incoming flow Mach number as long as $\delta < \delta_{det}$, where δ_{det} is the maximum angle for which the oblique shock wave can be attached to the wedge. For example, as claimed in their paper, when $\delta = 29$ and 35 deg, the induction distances are reduced to the order of a millimeter and a tenth of a millimeter, respectively. Consequently, when the reflecting wedge angles δ (but still smaller than δ_{det}) are large, it could be practically assumed that $\overline{OK} \rightarrow 0$, i.e., that the reactive shock wave emanates from the leading edge of the reflecting wedge.

A detonation wave is known to possess a complex three-dimensional structure.[11] Ignoring this structure, one may think of a detonation wave as a reaction zone in which a fast exothermic chemical reaction occurs, preceded by a shock wave. The burning reaction is triggered after a certain induction time by the strong pressure and temperature rise in the shock wave, whereas the latter is supported by the heat liberated in the reaction zone.

Different detonation wave models are available, depending upon the desired accuracy and the specific problem encountered. Usually, the chemical reaction zone will be very thin. Furthermore, the thickness of the induction zone will decrease exponentially with increasing temperature and may be ignored in a great many cases. Under these assumptions, the leading shock wave and the reaction zone are considered as a single discontinuity and give rise to the single-front model,[12] which is adopted in this study. This is the simplest theoretical description of a detonation wave. Consequently, the diffraction of a detonation wave could be expected to be similar to that of a nonreactive shock wave as long as the reaction zone is thin compared with any other length scale present in the flowfield.

In classical textbooks (e.g., Refs. 13 and 14), the development of the Hugoniot curve does not account for the fact that the value of the specific heat capacities ratio γ changes across the detonation wave as a result of the change in the components of the gas mixture and the increase of the temperature. The importance of taking different values of γ across detonation waves has been well recognized in the detonation/combustion literature, e.g., Ref. 15. This implies that as a first step of any such treatment, the two-γ Hugoniot curve of detonation waves should be developed. (For the reader's convenience, results of using the two-γ Hugoniot curve will be compared with the single-γ Hugoniot curve whenever necessary.)

Hugoniot Curve of Detonation Waves

Consider Fig. 2a, in which a detonation wave having a constant velocity U_D is seen to propagate from right to left toward a quiescent mixture of reactive gases, state (0), whose density, pressure, and enthalpy are ρ_0, P_0, and h_0, respectively. Based on the single-front model, adopted for this study, the chemical reaction takes place in an infinitely narrow reaction zone. The flowfield behind the reaction zone, state (1), which consists of a new mixture of gases, is in equilibrium and follows the detonation wave with the detonation-induced velocity u_1.

Because the detonation wave propagates with a constant velocity, a Galilean transformation can be performed on the unsteady flowfield, shown in Fig. 2a, to obtain the pseudosteady flowfield,

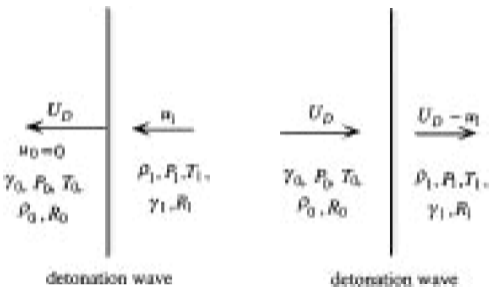

a) Unsteady coordinates b) Detonation fixed coordinates

Fig. 2 Schematic illustration of the detonation wave structure following the single front model.

shown in Fig. 2b, in detonation fixed coordinates. The conservation equations of mass, linear momentum, and energy for the pseudosteady flowfield, shown in Fig. 2b, are

$$\rho_0 U_D = \rho_1 (U_D - u_1) \tag{1}$$

$$P_0 + \rho_0 U_D^2 = P_1 + \rho_1 (U_D - u_1)^2 \tag{2}$$

$$h_0 + \tfrac{1}{2} U_D^2 = h_1 + \tfrac{1}{2} (U_D - u_1)^2 - q \tag{3}$$

If we further assume that the gas mixtures on both sides of the detonation zone consist of perfect gases, then the following relations hold:

$$h_j = c_{p_j} T_j, \qquad P_j = \rho_j R_j T_j, \qquad c_{p_j} = \frac{\sum_{k=1}^{N_j} n_{kj} m_{kj} c_{p_k}}{\sum_{k=1}^{N_j} n_{kj} m_{kj}}$$

$$c_{v_j} = \frac{\sum_{k=1}^{N_j} n_{kj} m_{kj} c_{v_j}}{\sum_{k=1}^{N_j} n_{kj} m_{kj}}, \qquad \gamma_j = \frac{c_{p_j}}{c_{v_j}}$$

$$R_j = c_{p_j} - c_{v_j} = \frac{\gamma_j - 1}{\gamma_j} c_{p_j}, \qquad a_j^2 = \frac{\gamma_j P_j}{\rho_j}$$

In the preceding relations, $j = 0$ and 1 for the flow states ahead (0) and behind (1) the detonation wave, respectively. The terms n_k and m_k are the mole number and the molecular mass, respectively, of the kth component of the gas mixture, which has in total N components.

Equations (1) and (2) can be combined to result in the Rayleigh line,

$$R = \frac{U_D^2}{V_0^2} - \frac{P_1 - P_0}{V_0 - V_1} = 0 \tag{4}$$

and Eqs. (1–3) can be combined to result in the Hugoniot line,

$$H = \left[(P_1/P_0) + \mu_1^2\right]\left[(V_1/V_0) - \mu_1^2\right] - \left[\left(\mu_1^2/\mu_0^2\right) - \mu_1^4 + 2\mu_1^2 (q/P_0 V_0)\right] = 0 \tag{5}$$

where $V = 1/\rho$ and $\mu^2 = (\gamma + 1)/(\gamma - 1)$.

Note that in many previous studies the postdetonation wave value of γ_1 was assigned, for simplicity reasons, to the flow state ahead of the detonation wave, i.e., $\gamma_0 = \gamma_1$; as a result, Eq. (5) assumed the form

$$\left[(P_1/P_0) + \mu^2\right]\left[(V_1/V_0) - \mu^2\right] = 1 - \mu^4 + 2\mu^2 (q/P_0 V_0) \tag{6}$$

which, for example, is identical to Eq. (2.9) in Ref. 13 (p. 18).

To solve the preceding equations, the value of q, i.e., the heat released in a complete reaction, must be determined. This can be done by either measuring it or relating it to other parameters that are assumed to be the initial conditions. The latter approach is used in the present study. This is done by introducing the Chapman–Jouguet (CJ) condition, which corresponds to the point where the Hugoniot

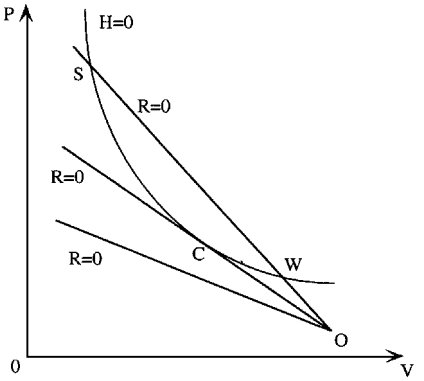

Fig. 3 Rayleigh (R) and Hugoniot (H) curves in the (P, V) plane.

curve [Eq. (5)] is tangent to the Rayleigh curve [Eq. (4)], as shown in Fig. 3. By combining Eqs. (4) and (5), one obtains

$$\left(U_D^2/P_0 V_0\right)(V_1/V_0)^2 - \left\{\left[1 + \mu_1^2 + \left(U_D^2/P_0 V_0\right)\right] + \mu_1^2\left(U_D^2/P_0 V_0\right)\right\}(V_1/V_0) + \mu_1^2\left[1 + \mu_1^2 + \left(U_D^2/P_0 V_0\right)\right] + \left(\mu_1^2/\mu_0^2\right) - \mu_1^4 - 2\mu_1^2 (q/P_0 V_0) = 0 \tag{7}$$

The point of tangency C can be found by finding the conditions for which the discriminant of Eq. (7) is zero. Under the CJ condition, i.e., $U_D = U_{\mathrm{CJ}}$,

$$M_{\mathrm{CJ}} = U_{\mathrm{CJ}}/a_0 \tag{8}$$

where

$$a_0^2 = \gamma_0 (P_0/\rho_0) = \gamma_0 P_0 V_0 = \gamma_0 R_0 T_0 \tag{9}$$

Inserting Eqs. (8) and (9) into the discriminant of Eq. (7) and solving for q results in

$$q = \frac{a_0^2}{2\gamma_0^2(\gamma_0 - 1)\left(\gamma_1^2 - 1\right)M_{\mathrm{CJ}}^2} \times \left[\gamma_1^2(\gamma_0 - 1) + 2\gamma_0\left(\gamma_0 - \gamma_1^2\right)M_{\mathrm{CJ}}^2 + \gamma_0^2(\gamma_0 - 1)M_{\mathrm{CJ}}^4\right] \tag{10}$$

where a_0, γ_0, γ_1, and M_{CJ} are assumed to be known. Note that the preceding model assumes that the gases on both sides of the detonation wave are perfect and hence q is assumed to be independent of the temperature. If again the assumption that $\gamma_0 = \gamma_1 = \gamma$ is used, then Eq. (10) reduces to

$$q^* = \frac{a_0^2\left(1 - M_{\mathrm{CJ}}^2\right)^2}{2(\gamma^2 - 1)M_{\mathrm{CJ}}^2} \tag{11}$$

which for the strong shock assumption, i.e., $M_{\mathrm{CJ}} \gg 1$, yields

$$q^* = \frac{M_{\mathrm{CJ}}^2 a_0^2}{2(\gamma^2 - 1)} = \frac{U_{D\mathrm{CJ}}^2}{2(\gamma^2 - 1)} \tag{12}$$

Note again that, although the general solution for q is given by Eq. (10), the forms given by Eq. (11) or (12) have been used in other studies owing to the unjustified use of the oversimplifying assumption that $\gamma_0 = \gamma_1 = \gamma$. Equations (11) and (12) prevail in many classical textbooks (see Ref. 13, p. 54).

The insertion of q from Eq. (10), which accounts for the fact that $\gamma_0 \neq \gamma_1$, into Eq. (3) results in a set of three equations [Eqs. (1–3)], with three unknowns ρ_1, P_1, and h_1 (T_1 actually), provided the chemical reaction, which is needed to calculate the parameters c_p, c_v, γ, and R [with the aid of the relations following Eq. (3)], is known. The solution of these equations, which satisfies the CJ condition, is simple and straightforward, although somewhat cumbersome, as shown in the next section.

Note here that, as shown in Fig. 3, the velocity, or Mach number, of a steady detonation wave cannot be smaller than the detonation velocity at the CJ point, i.e., $M \geq M_{\mathrm{CJ}}$. The ratio between the actual detonation wave velocity and that calculated by the CJ condition is known as the overdrive and is denoted in the present work as $\alpha = M/M_{\mathrm{CJ}}$. More details can be found in Ref. 13.

Normal Detonation Wave Relations

By combining Eqs. (1–3) and using thermodynamic relations, one can get

$$u_1^2 + \frac{2a_0}{\gamma_1+1}\left(\frac{\gamma_1}{\gamma_0}\frac{1}{M} - M\right)u_1 + \frac{2(\gamma_1-1)}{\gamma_1+1}\left[q + \frac{(\gamma_1-\gamma_0)a_1^2}{\gamma_0(\gamma_0-1)(\gamma_1-1)}\right] = 0 \tag{13}$$

where $M = U_D/a_0$. [Recall that q is given by Eq. (10).] Solving Eq. (13) results in the detonation-induced flow velocity

$$u_1/a_0 = [(1+\beta)/(\gamma_1+1)][M - (\gamma_1/\gamma_0)(1/M)] \tag{14}$$

where

$$\beta = \left[1 - \frac{2(\gamma_1^2-1)M^2(\bar{q}+\eta)}{(M^2-\gamma_1/\gamma_0)^2}\right]^{\frac{1}{2}} \tag{15a}$$

$$\eta = \frac{(\gamma_1-\gamma_0)}{\gamma_0(\gamma_0-1)(\gamma_1-1)} \tag{15b}$$

and

$$\bar{q} = q/a_0^2 \tag{15c}$$

Note again that, if the assumption $\gamma_0 = \gamma_1 = \gamma$ is used, then Eq. (15b) results in $\eta = 0$. Inserting this value into Eq. (15a) yields

$$\beta^* = \left[1 - \frac{2(\gamma^2-1)M^2\bar{q}}{(M^2-1)^2}\right]^{\frac{1}{2}} \tag{16a}$$

which is identical to Eq. (2) in Ref. 16 and that given in many textbooks that, instead of Eq. (14), incorrectly suggest the following relation, which is not general as it is limited to $\gamma_0 = \gamma_1 = \gamma$:

$$u_1/a_0 = [(1+\beta^*)/(\gamma+1)][M - (1/M)] \tag{16b}$$

The ratios of the densities, the pressures, the sound speeds, and the temperatures across the detonation wave can be obtained as follows:

$$\frac{\rho_1}{\rho_0} = \frac{U_D}{U_D-u_1} = \frac{M}{M - [(1+\beta)/(\gamma_1+1)][M-(\gamma_1/\gamma_0)(1/M)]} = \frac{(\gamma_1+1)M^2}{(\gamma_1-\beta)M^2 + (1+\beta)(\gamma_1/\gamma_0)} \tag{17}$$

$$\frac{P_1}{P_0} = \frac{(1+\beta)\gamma_0 M^2 - \gamma_1\beta + 1}{\gamma_1+1} \tag{18}$$

$$\frac{a_1}{a_0} = \frac{\left((1+\beta)\gamma_1 M^2 - \{[\gamma_1(\gamma_1\beta-1)]/\gamma_0\}\right)^{\frac{1}{2}}\left((\gamma_1-\beta)M^2 + \{[\gamma_1(1+\beta)]/\gamma_0\}\right)^{\frac{1}{2}}}{(\gamma_1+1)M} \tag{19}$$

$$T_1/T_0 = (\gamma_0 R_0/\gamma_1 R_1)(a_1/a_0)^2 \tag{20}$$

By setting $\gamma_0 = \gamma_1 = \gamma$ and $q = 0$, i.e., no reaction, relations (14), (17), (18), and (19) reduce, as expected, to the Rankine–Hugoniot relations across normal shock waves.

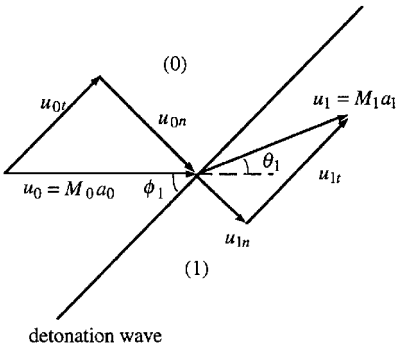

Fig. 4 Schematic illustration of a steady oblique detonation wave and definition of flow parameters.

Oblique Detonation Wave Relations

In the following the oblique detonation wave is again treated using the single-front model. Note that this model was termed by Fickett and Davis[13] as the "simplest model."

A steady oblique detonation wave is shown schematically in Fig. 4. The flow states ahead and behind the oblique detonation wave are (0) and (1), respectively. The angle of incidence between the oncoming supersonic flow and the oblique detonation wave is ϕ_1. While passing through the oblique detonation wave, the flow is deflected by an angle θ_1. Denoting the steady velocities ahead and behind the detonation wave as U_0 and U_1, respectively, and solving the flowfield in a coordinate system normal (n) and tangential (t) to the oblique detonation wave, in a way similar to that done with oblique shock waves,[17] results in

$$\frac{U_1}{a_0} = \left\{M_0^2\left[1 + \frac{(1+\beta)(\beta-1-2\gamma_1)}{(\gamma_1+1)^2}\sin^2\phi_1\right] - \frac{2\gamma_1(1+\beta)(\beta-\gamma_1)}{\gamma_0(1+\gamma_1)^2} + \left(\frac{1+\beta}{\gamma_1+1}\right)^2\left(\frac{\gamma_1}{\gamma_0}\right)^2\frac{1}{M_0^2\sin^2\phi_1}\right\}^{\frac{1}{2}} \tag{21}$$

where $M_0 = U_0/a_0$. The postdetonation wave flow Mach number M_1 is defined as $M_1 = U_1/a_1$, where the postdetonation speed of sound a_1 can be simply obtained from Eq. (19) to read

$$\frac{a_1}{a_0} = \frac{\left((1+\beta)\gamma_1 M_0^2\sin^2\phi_1 - \{[\gamma_1(\gamma_1\beta-1)]/\gamma_0\}\right)^{\frac{1}{2}}\left((\gamma_1-\beta)M_0^2\sin^2\phi_1 + \{[\gamma_1(1+\beta)]/\gamma_0\}\right)^{\frac{1}{2}}}{(\gamma_1+1)M_0\sin\phi_1} \tag{22}$$

Similarly, β as obtained from Eq. (15a) is

$$\beta = \left\{1 - \frac{2(\gamma_1^2-1)M_0^2\sin^2\phi_1(\bar{q}+\eta)}{\left[M_0^2\sin^2\phi_1 - (\gamma_1/\gamma_0)\right]^2}\right\}^{\frac{1}{2}} \tag{23}$$

The flow deflection angle θ_1 is given by

$$\theta_1 = \phi_1 - \arctan\left[\frac{\gamma_1-\beta}{\gamma_1+1}\tan\phi_1 + \frac{2\gamma_1(1+\beta)}{\gamma_0(\gamma_1+1)M_0^2\sin 2\phi_1}\right] \tag{24}$$

The maximum flow deflection angle condition, i.e., $(\partial\theta_1/\partial\phi_1)|_{M_0} = 0$, results in

$$A\sin^4\phi_1 + B\sin^2\phi_1 + C = 0 \tag{25}$$

where

$$A = \gamma_0^2[\beta(\beta^2+\beta-1) - 1 - \gamma_1(1+\beta)^2]M_0^4 \tag{26a}$$

$$B = \gamma_0(1+\beta)\big[\gamma_0(1+\gamma_1)(\beta+\gamma_0-\beta\gamma_0)M_0^2 - \gamma_1(1+\beta+2\beta^2)\big]M_0^2 \quad (26b)$$

$$C = \gamma_1(1+\beta)\big[\gamma_1\beta(1+\beta)+\gamma_0(1+\gamma_1)M_0^2\big] \quad (26c)$$

By solving Eqs. (25) and (26), one gets

$$\sin^2\phi_{1,\mathrm{det}} = f(\gamma_0, \gamma_1, M_{\mathrm{CJ}}, M_0) \quad (27)$$

If $\gamma_0 = \gamma_1 = \gamma$ and $q = 0$ are assumed, then Eq. (27) reduces, as expected, to the well-known relation appropriate to oblique shock waves in nonreactive gases (see Ref. 18, p. 370), i.e.,

$$\sin^2\phi_{1,\mathrm{det}} = \big(1/\gamma M_0^2\big)\Big([(\gamma+1)/4]M_0^2 - 1 + \big[(\gamma+1)\big\{1+[(\gamma-1)/2]M_0^2+[(\gamma+1)/16]M_0^4\big\}\big]^{\frac{1}{2}}\Big) \quad (28)$$

Now that the governing equations associated with an oblique detonation wave have been developed, they can be used to solve some classical problems and verified by comparing the analytical with experimental and numerical results.

Supersonic Flow of a Reactive Gas Mixture Past a Wedge

Figure 1b is a schematic illustration of the flowfield that is developed when a supersonic flow of a mixture of reactive gases encounters a sharp wedge whose angle δ is smaller than the detachment angle δ_{det}. If the flow properties in state (0) are given and the chemical reaction has the form

$$\sum_{j=1}^{N_0} n_j X_j = \sum_{k=1}^{N_1} n_k X_k \quad (29)$$

where X denotes a gas component, N_0 and N_1 are the number of the gas components of which the gas mixtures in states (0) and (1) consist. Then the flow constants in state (1), i.e., γ_1 and R_1, can be calculated using the relations that are listed following Eq. (3).

Once these constants are known, the angle of incidence ϕ_1 can be obtained by solving Eq. (24) for $\theta_1 = \delta$. The knowledge of ϕ_1, together with the known parameters ahead of the detonation front, is sufficient to calculate both the dynamic and the thermodynamic postoblique detonation wave flow properties with the aid of the equations developed in the previous sections. The angle of incidence appropriate to the detachment point, $\phi_{1,\mathrm{det}}$, is obtained by solving Eq. (27), and the maximum flow deflection wedge angle, i.e., δ_{det}, is obtained by inserting the value of $\phi_{1,\mathrm{det}}$ into Eq. (24).

The values of γ_0, γ_1, and $a_0(X)/a_0\,(X=0)$ for the mixture $2H_2 + O_2 + X\mathrm{Ar}$ and five different values of X are shown in Table 2. Note that the values of γ_1 in Table 2 were calculated by accounting for the fact that the postdetonation wave temperature is much higher than that ahead of it. The value of γ_1 for $X=0$ was taken from Ref. 9, which used the Gordon–McBride[19] code. The other values of γ_1 were simply calculated by accounting for the argon with $\gamma = \frac{5}{3}$ and its appropriate concentration in the mixture, i.e., the value of X. (Note that in the preceding procedure it is assumed that the value of γ for argon is independent of the postdetonation temperature in the range of the temperatures associated with the present chemical reactions.) To illustrate the effect of the high temperature on γ_1, the values of γ_1 were also calculated without accounting for the postdetonation wave temperature. These values are marked in Table 2 as γ_1^*. It is evident from Table 2 that using a single-γ model for small values of X might introduce large errors. For example,

Table 2 Mixture properties as a function of X for the mixture $2H_2 + O_2 + X\mathrm{Ar}$

	X				
	0	1	2	5	7
γ_0	1.402	1.54	1.58	1.62	1.63
γ_1	1.13	1.41	1.49	1.58	1.60
γ_1^*	1.333	1.50	1.55	1.61	1.62
$[a_0(X)/a_0(0)]$	1	0.806	0.739	0.668	0.650

Table 3 Dependence of ϕ_1 and δ for inert and reactive $2H_2 + O_2 + 3.76\,N_2$

	δ, deg		
	20	25	30
ϕ_1^{inert}	26.6	32.7	39.2
$\phi_1^{\mathrm{reactive}}$	44.5	49.0	55.9

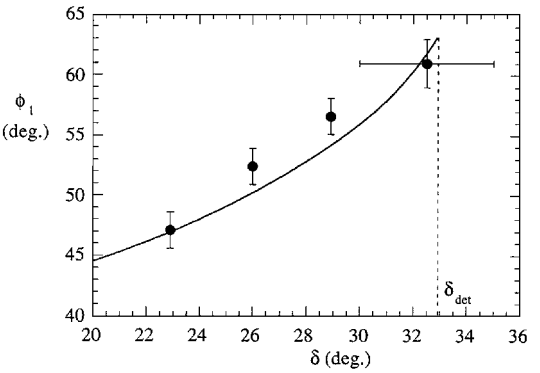

Fig. 5 Dependence of the angle of incidence of the detonation wave ϕ_1 on the flow deflection angle δ: ●, numerical calculations and ——, current analytical prediction for $M_0 = 8$, $M_{\mathrm{CJ}} = 5.4$, and $\gamma_1 = 1.32$.

for $X = 0$, $\gamma_0 = 1.402$ and $\gamma_1 = 1.13$. It is also evident from Table 2 that accounting for the postdetonation wave temperature is important for small values of X. Again for $X = 0$, $\gamma_1 = 1.13$, whereas $\gamma_1^* = 1.333$. The differences between γ_0, γ_1, and γ_1^* become very small at $X = 7$, where we have $\gamma_0 = 1.63$, $\gamma_1 = 1.60$, and $\gamma_1^* = 1.62$.

Calculation, based on the foregoing proposed model, of the dependence of the angle of incidence ϕ_1 on the flow deflection angle δ for a supersonic flow having a Mach number M_0 of the gas mixture ($M_{\mathrm{CJ}} = 5.4$) is shown in Fig. 5 as a solid line. The value of γ_1 used in the calculation was 1.32 as reported by Gelfand et al.[1] Four numerically calculated points, by Li et al.,[10] who used a single-γ model, are added to Fig. 5. Accounting for the vertical error bars associated with the numerical data indicates that the agreement between their numerical data and our analytical calculations is good. The maximum flow deflection angle δ_{det} as calculated theoretically using the model proposed in this study was 32.9 deg and is shown by the vertical dashed line in Fig. 5. This value is in excellent agreement with the value obtained numerically by Li et al.,[10] who reported a value of 32.5 deg ± 2.5 deg (see the horizontal error bar in Fig. 5). Note that a single-γ calculation, i.e., $\gamma_0 = \gamma_1 = 1.32$, would result in a line slightly lower than the one shown in Fig. 5, where $\gamma_0 = 1.4$ and $\gamma_1 = 1.32$. The difference between the two lines depends on the nitrogen dilution, as mentioned earlier when Table 2 was discussed.

To the best of the authors' knowledge, this is the first time that an accurate enough analytical model for calculating oblique detonation waves has been presented. Li et al.[10] presented numerical calculations. Owing to the renewed interest in using oblique steady detonations as a combustion mechanism in high-speed-propulsion devices, it is important to develop accurate analytical models for standing oblique detonation waves.

A comparison between reactive and inert (nonreactive) calculations of the dependence of ϕ_1 on δ for the reactive mixture $2H_2 + O_2 + 3.76N_2$ at $M_0 = 8$, $M_{\mathrm{CJ}} = 5.4$, $\gamma_0 = 1.4$, and $\gamma_1 = 1.32$ is shown in Table 3. As can be seen, $\phi_1^{\mathrm{reactive}} > \phi_1^{\mathrm{inert}}$ by about 17 deg ± 1 deg for $20 < \delta < 30$ deg. In addition, whereas for the case of an inert flow $\delta_{\mathrm{det}}^{\mathrm{inert}} = 43.8$ deg, for the case of reactive flow $\delta_{\mathrm{det}}^{\mathrm{reactive}} = 32.9$ deg. Note that the appropriate values of $\phi_{1,\mathrm{det}}$ as calculated, i.e., $\phi_{1,\mathrm{det}}^{\mathrm{inert}} = 67.5$ deg and $\phi_{1,\mathrm{det}}^{\mathrm{reactive}} = 63.1$ deg, are closer.

Detonation Wave Reflection

Owing to the similar gasdynamics nature of detonation and shock waves, planar detonation waves also reflect as either a regular or a MR when they interact with an oblique wedge. Because the wave

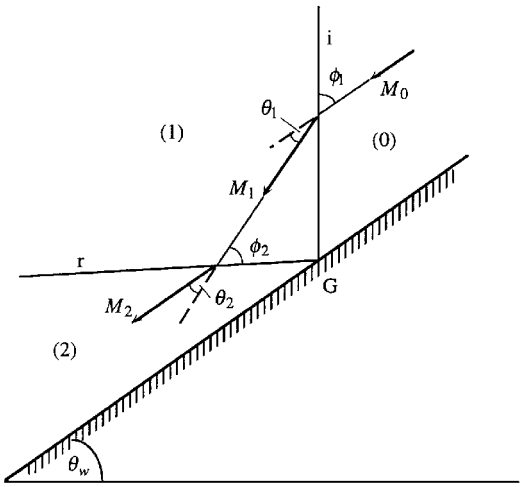

Fig. 6 Schematic illustration of the wave configuration of a RR and definition of the flow parameters.

configurations of both regular and MRs consist of oblique detonation waves, and because, as shown in the preceding section, the currently proposed analytical model for an oblique detonation wave seems to be correct, a natural step is to develop theories similar to the two- and three-shock theories for detonation waves. This indeed is done in the following two sections.

Regular Reflection of Detonation Waves

The wave configuration of a RR is shown schematically in Fig. 6. In detonation fixed coordinates, the reactive gas mixture in state (0) flows with a Mach number M_0 and encounters the detonation wave i. The angle of incidence is ϕ_1. As a result, the chemical reaction is initiated, and immediately behind the incident detonation wave, there is a new gas mixture. The new conditions of the gas mixture can be calculated by the procedure outlined in the previous section. Because the gas in state (1) is not reactive anymore, the reflected wave r is a shock wave and not a detonation wave.

The flow deflection across the detonation wave i can be written as

$$\theta_1 = G_D(\gamma_0, \gamma_1, M_{CJ}, M_0, \phi_1) \tag{30}$$

where the function G_D can be obtained from Eq. (24):

$$G_D = G_D(\gamma_i, \gamma_j, M_{CJ}, M, \phi) = \phi - \arctan\left[\frac{\gamma_j - \beta}{\gamma_j + 1}\tan\phi + \frac{2\gamma_j(1+\beta)}{\gamma_i(\gamma_j+1)M^2\sin 2\phi}\right] \tag{31}$$

The flow Mach number of the gas mixture in state (1) can be written as

$$M_1 = F_D(\gamma_0, \gamma_1, M_{CJ}, M_0, \phi_1) \tag{32}$$

where the function F_D can be obtained from Eqs. (22) and (23):

$$F_D = F_D(\gamma_i, \gamma_j, M_{CJ}, M, \phi) = \frac{(\gamma_j+1)M\sin\phi}{\left((1+\beta)\gamma_j M^2\sin^2\phi - \{[\gamma_j(\gamma_j\beta-1)]/\gamma_i\}\right)^{\frac{1}{2}}\left((\gamma_j-\beta)M^2\sin^2\phi + \{[\gamma_j(\gamma_j\beta-1)]/\gamma_i\}\right)^{\frac{1}{2}}} \times \left\{M^2\left[1 + \frac{(1+\beta)(\beta-1-2\gamma_j)}{(\gamma_j+1)^2}\sin^2\phi\right] - \frac{2\gamma_j(1+\beta)(\beta-\gamma_j)}{\gamma_i(1+\gamma_j)^2} + \frac{(1+\beta)^2\gamma_j^2}{(\gamma_j+1)^2\gamma_i^2M^2\sin^2\phi}\right\}^{\frac{1}{2}} \tag{33}$$

The initial conditions imply that

$$\phi_1 = (\pi/2) - \theta_w \tag{34}$$

and

$$M_0 = \frac{M_i}{\sin\phi_1} = \frac{M_i}{\cos\theta_w} \tag{35}$$

The reflected shock wave r can be treated similarly. The flow deflection across the reflected shock wave can be expressed as

$$\theta_2 = G_S(\gamma_1, M_1, \phi_2) \tag{36}$$

where

$$G_S = G_S(\gamma, M, \phi) = \arctan\left[2\cot\phi\frac{M^2\sin^2\phi - 1}{M^2(\gamma + \cos 2\phi) + 2}\right] \tag{37}$$

The flow Mach number of the gas mixtures in state (2) can be expressed as

$$M_2 = F_S(\gamma_1, M_1, \phi_2) \tag{38}$$

where

$$F_S = F_S(\gamma, M, \phi) = \frac{(1 + (\gamma-1)M^2\sin^2\phi + \{[(\gamma+1)/2]^2 - \gamma\sin^2\phi\}M^4\sin^2\phi)^{\frac{1}{2}}}{\{\gamma M^2\sin^2\phi - [(\gamma-1)/2]\}^{\frac{1}{2}}\{[(\gamma-1)/2]M^2\sin^2\phi + 1\}^{\frac{1}{2}}} \tag{39}$$

The boundary condition for a RR is

$$\theta_1 - \theta_2 = 0 \tag{40}$$

Equations (30), (32), (36), (38), and (40) contain five unknowns, namely, θ_1, θ_2, M_1, M_2, and ϕ_2, and hence are solvable, in principle.

By replacing Eq. (38) with the following equation, which is simply obtained from Eq. (28):

$$\sin^2\phi_{1,det} = \frac{1}{\gamma_1 M_1^2}\left\{\frac{\gamma_1+1}{4}M_1^2 - 1 + \left[(\gamma_1+1)\left(1 + \frac{\gamma_1-1}{2}M_1^2 + \frac{\gamma_1+1}{16}M_1^4\right)\right]^{\frac{1}{2}}\right\} \tag{41}$$

one obtains a somewhat different set of five equations, namely, Eqs. (30), (32), (36), (40), and (41), which again contain five unknowns, namely, θ_1, θ_2, M_1, M_2, and $\phi_{1,det}$. The solution of this set will result in the angle of incidence of the detonation wave $\phi_{1,det}$ being appropriate to the well-known detachment criterion,[17] at which the transition from regular to MR takes place. The corresponding reflecting wedge angle can then be calculated from Eq. (34), i.e., $\theta_w^{tr}(RR \leftrightarrow MR) = \pi/2 - \phi_{1,det}$.

The transition wedge angle $\theta_w^{tr}(RR \leftrightarrow MR)$, calculated using this method for the mixture $2H_2 + O_2 + X$Ar, is shown in Table 4 for five different values of X and three different values of overdrive of the incident detonation wave, $\alpha_i = M_i/M_{CJ}$. The values of θ_w^{tr} increase both with X and α_i. The calculations at the CJ point were done with and without accounting for the dependence of γ_1 on the postdetonation temperature. As mentioned earlier, the difference between these calculation becomes more significant as the values of X decreases. A 1% overdrive ($\alpha_i = 1.01$) strongly affects the transition wedge angles. Note that the values of θ_w^{tr} increase by 5 deg for all the values of X when a 1% overdrive is assumed. If a 10% overdrive ($\alpha_i = 1.1$) is assumed, then the values of θ_w^{tr} increase by about 10 deg. Hence, it is clear that the process is nonlinear.

The values that were calculated by the method developed here (Table 4) seem to agree well with those measured experimentally by different investigators (Table 1). The scatter in the experimental results could be explained in the changes in both X and α_i and the

Table 4 RR ↔ MR transition wedge angle for $2H_2 + O_2 + XAr$

	X				
	0	1	2	5	7
$\theta_w^{tr}(\alpha_i = 1)$, deg	33.68	36.73	37.45	38.18	38.33
$\theta_w^{tr}(\alpha_i = 1)^a$, deg	35.95	37.53	37.94	38.41	38.38
$\theta_w^{tr}(\alpha_i = 1.01)$, deg	38.22	41.47	42.21	42.97	43.13
$\theta_w^{tr}(\alpha_i = 1.1)$, deg	42.83	46.87	47.75	48.63	48.81

[a]Without accounting for the postdetonation temperature

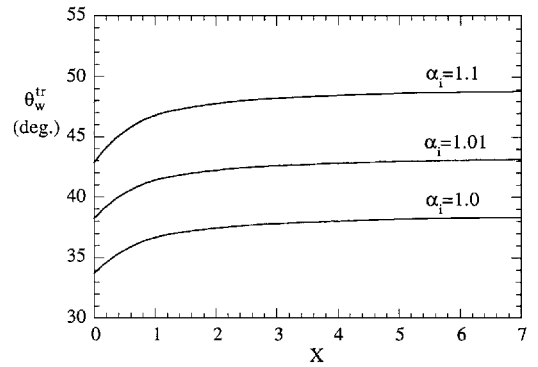

Fig. 7 Dependence of the RR ↔ MR transition wedge angle θ_w^{tr} on X of the mixture $2H_2 + O_2 + XAr$ for three diferent values of overdrive, α_i.

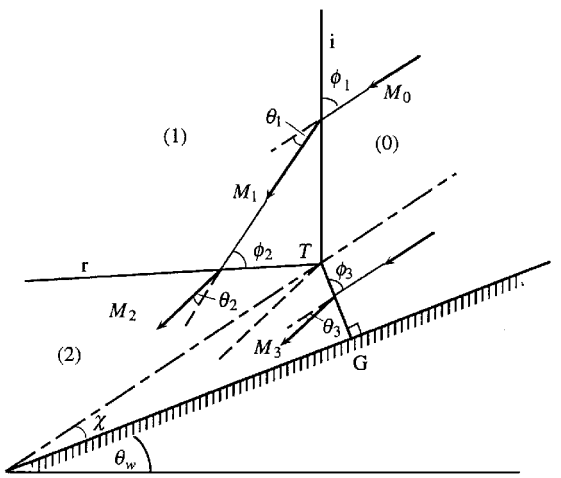

Fig. 8 Schematic illustration of the wave configuration of a MR and definition of the flow parameters.

different cell sizes in the various experiments. The dependence of θ_w^{tr} on X for different overdrives is also given in Fig. 7, which is calculated by the present model. Note again that, in the calculations shown in Fig. 7, the dependence of γ_1 on the postdetonation wave temperature was accounted for.

MR of Detonation Waves

A schematic illustration of a MR with the definition of the relevant flow parameters is shown in Fig. 8. The incident wave i and the Mach stem m are detonation waves. Immediately behind them the chemical reaction is over, and hence the reflected wave r is a shock wave. In addition, because the incident detonation wave velocity is close to the CJ velocity, the Mach stem, whose velocity is larger than the incident detonation wave velocity, is an overdriven detonation wave. For this reason, MR wave configurations have been used in the past to study overdriven detonation waves.[6]

The governing equations across the detonation waves i and m can be written as

$$\theta_j = G_D(\gamma_0, \gamma_j, M_{CJ}, M_0, \phi_j) \tag{42}$$

$$M_j = F_D(\gamma_0, \gamma_j, M_{CJ}, M_0, \phi_j) \tag{43}$$

$$P_j = P_0 H_D(\gamma_0, \gamma_j, M_{CJ}, M_0, \phi_j) \tag{44}$$

where for the incident detonation wave $j = 1$ and for the Mach stem detonation wave $j = 3$. The functions G_D and F_D are given by Eqs. (31) and (33), respectively, and the function H_D can be simply obtained from Eq. (18) to read

$$H_D = H_D(\gamma_i, \gamma_j, M_{CJ}, M, \phi) = \frac{(1+\beta)\gamma_i M^2 \sin^2\phi - \gamma_j\beta + 1}{\gamma_j + 1} \tag{45}$$

Assuming that the Mach stem is straight and normal to the reflecting surface and that the triple point propagates along a straight line emanating from the leading edge of the reflecting wedge, the following geometrical relations are self-explanatory:

$$\phi_1 = (\pi/2) - (\theta_w + \chi) \tag{46}$$

$$\phi_3 = (\pi/2) - \chi \tag{47}$$

Here χ is the triple point trajectory angle. Note that, as mentioned by Ben-Dor,[17] the preceding assumptions, which are essential for proceeding with the development, are known to be good in a large range of parameters.

In addition, the pseudosteady flow Mach number in state (0) can be obtained from

$$M_0 = \frac{M_i}{\sin\phi_1} = \frac{M_i}{\cos(\theta_w + \chi)} \tag{48}$$

Similar to the foregoing presentation, the governing equations across the reflected shock wave r are

$$\theta_2 = G_S(\gamma_1, M_1, \phi_2) \tag{49}$$

$$M_2 = F_S(\gamma_1, M_1, \phi_2) \tag{50}$$

and

$$P_2 = P_1 H_S(\gamma_1, M_1, \phi_2) \tag{51}$$

The functions G_S and F_S are given by Eqs. (37) and (39), respectively, and the function H_S is

$$H_S = H_S(\gamma, M, \phi) = [2/(\gamma+1)]\{\gamma M^2 \sin^2\phi - [(\gamma-1)/2]\} \tag{52}$$

The flows passing through the incident detonation wave i and the Mach stem detonation wave m undergo the same chemical reactions; therefore if the dependence of γ on the temperature is ignored (see subsequent justification), $\gamma_1 = \gamma_3$. In addition, because the reflected wave is not a detonation wave but a shock wave and because it is a moderate shock wave ($M_r < 2$), the value of γ practically does not change as the flow passes across it from state (1) to state (2), and hence $\gamma_2 = \gamma_1$.

Combining the preceding two relations implies that, behind the detonation front that consists of i and m, the entire flowfield can be assumed to have the same value of γ, i.e., $\gamma_1 = \gamma_2 = \gamma_3$. The matching conditions across the slipstream s are

$$\theta_1 - \theta_2 = \theta_3 \tag{53}$$

and

$$P_2 = P_3 \tag{54}$$

This set of 12 equations, namely, Eqs. (42), (43), and (44) for $j = 1$ and 3 and Eqs. (47), (49–51), (53), and (54), contains 12 unknowns: $\theta_1, \theta_2, \theta_3, P_1, P_2, P_3, M_1, M_2, M_3, \phi_2, \phi_3$, and χ. Consequently, the set is complete and can, in principle, be solved.

Comparison of the Analytical Predictions with the Experimental Results

The experimental results of Meltzer et al.[2] on the variation of the triple point trajectory angle χ with the reflecting wedge angle θ_w for detonations in $2H_2 + O_2$ mixture at 288 K and 0.2 bar are shown in Fig. 9. Their calculation (dashed line) was based on a model they called the three-shock-theory. The solid lines are calculations based on the present model with $\gamma_0 = 1.4$, $\gamma_1 = \gamma_2 = \gamma_3 = 1.13$ (Ref. 9), and $M_{CJ} = 5.1$ (Ref. 2). The calculations at the CJ point, i.e., $\alpha_i = 1$, yield results similar to those of Meltzer et al.[2] Both calculations underpredicted the triple point trajectory angles χ. An improvement

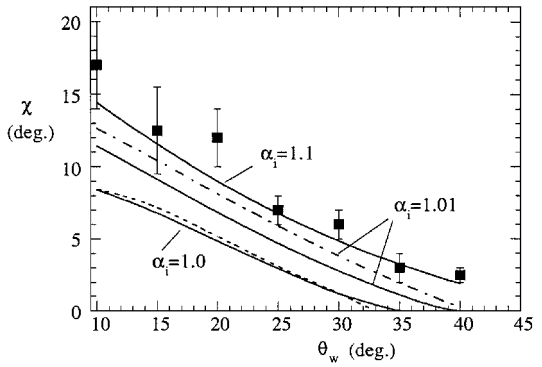

Fig. 9 Comparison of the analytical and experimental triple point trajectory angles for detonations in $2H_2 + O_2$ mixtures with predictions based on the current model.

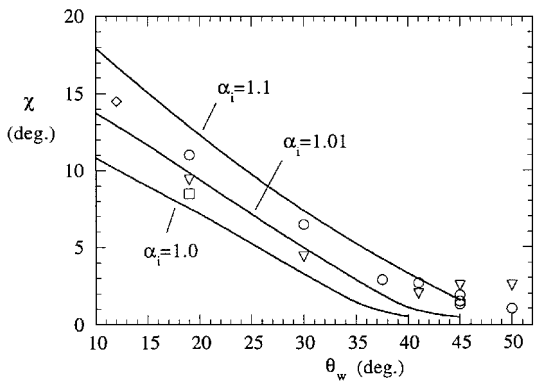

Fig. 10 Comparison of the experimental triple point trajectory angles for detonations in 30% $(2C_2H_2 + 5O_2) + 70\%$ Ar with predictions based on the current model.

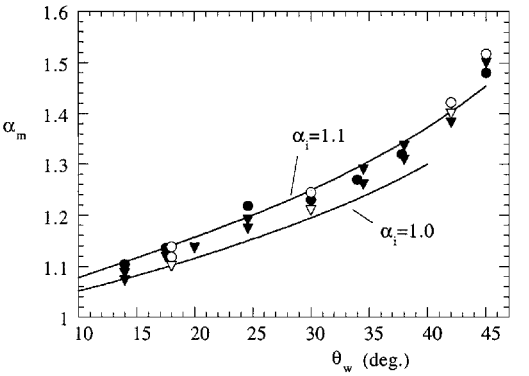

Fig. 11 Comparison of the experimental Mach stem overdrive for detonations in 30% $(2C_2H_2 + 5O_2) + 70\%$ Ar with predictions based on the current model.

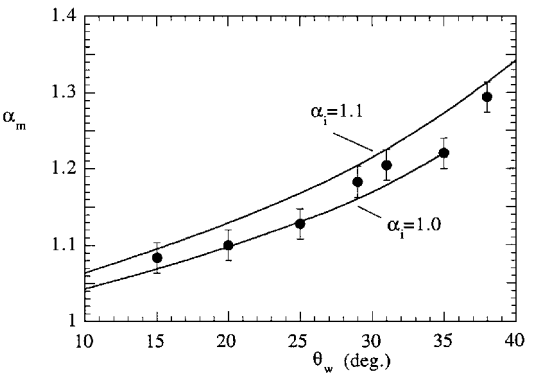

Fig. 12 Comparison of the experimental Mach stem overdrive for detonation in $2H_2 + O_2$ with predictions based on the current model.

of the analytical predictions is evident when an overdrive is assumed. As can be seen, even a 1% overdrive, i.e., $\alpha_i = 1.01$, results in a significant improvement. The dashed-dotted line in Fig. 9 is a result of a calculation with $\alpha_i = 1.01$ but without accounting for the postdetonation wave temperature, i.e., $\gamma_0 = 1.4$ and $\gamma_1 = \gamma_2 = \gamma_3 = 1.33$. The difference between the two calculations is about 1–2 deg.

The fact that χ is very sensitive to the degree of overdrive α_i and that the agreement of the analytical predictions with the experiments is not good enough can be explained as follows. The present study is based on the simple single-front model. The detonation front has in reality a cellular structure. As experimentally observed by Gavrilenko and Prokhorov,[7] the cell size of a detonation is very sensitive to α_i and drastically decreases as α_i increases. Edwards et al.'s[5] experiments clearly showed that the trajectory angle is strongly influenced by the cell size, especially for small wedge angles. The single-front model assumes that the cell size is infinitesimal and hence completely neglects the cell size influence. As can be expected, the smaller is the cell size, the smaller is the error introduced by the single front model.

Also note here that the values of α_i used in the experiments shown in Fig. 9 were claimed by the authors to be unity, i.e., CJ detonations. However, there are some doubts on this issue. Meltzer et al.'s[2] estimation of M_i as a CJ detonation was based on the comparison of their measured wave velocity and pressure with known CJ conditions. The measured wave velocity as obtained by them was consistently equal to 95–98% of the calculated CJ velocity. The fact that the measured wave velocity was smaller than the calculated value can be explained as the real detonation velocity deficit.[1] It is evident that there remains some uncertainty regarding the exact value of M_i. Consequently, slightly overdriven M_i is practically possible. A 1% overdrive of the incident detonation wave can result in a pronounced difference in χ.

Similar results but for detonations in 30% $(2C_2H_2 + 5O_2) +$ 70% Ar, which were reported by Edwards et al.,[5] are shown in Fig. 10. The analytical results (solid curves) were calculated by the present model using three different values of overdrive α_i. In these calculations, $\gamma_1 = \gamma_2 = \gamma_3 = 1.57$ (Ref. 1) and $M_{CJ} = 5.5$ (Ref. 5). The experimental data are seen, in general, to lie again between the calculations for $\alpha_i = 1.0$ and 1.1, close to the line appropriate to $\alpha_i = 1.01$.

The experimental results of Edwards et al.[5] for detonations in the mixture 30% $(2C_2H_2 + 5O_2) + 70\%$ Ar with different initial pressure conditions are shown in Fig. 11, which shows the dependence of the overdrive of the Mach stem, $\alpha_m = M_m/M_i$, on the reflecting wedge angle θ_w. The experimental results lie again between the analytical predictions for $\alpha_i = 1.0$ and 1.1. Figure 12 shows similar good agreement between the analytical predictions and the experimental results of Gavrilenko and Prokhonov[6] for detonations in the mixture $2H_2 + O_2$.

Conclusions

The conservation equations across an oblique detonation wave have been developed by considering different specific heat ratios γ on both sides of the detonation wave. Analytical predictions for steady oblique detonation waves were compared with numerical results, and in view of the complex phenomenon, good agreement was evident.

The developed conservation equations for oblique detonation waves were then used to construct appropriate two- and three-shock-theory-based models for describing the regular and the MR of detonation waves. Analytical predictions based on the two-shock theory of the RR ↔ MR transition wedge angles and those based on the three-shock theory of both the triple point trajectory angle and the Mach stem overdrive were compared with experimental results from various sources, and in general good agreement was evident.

The MR computations are novel and should provide stimulus to other researchers either to accept the explanation provided here for the disagreement between experiment and theory or to generate an alternate theory.

References

[1]Gelfand, B. E., Forolov, S. M., and Nettleton, M. A., "Gaseous Detonations—A Selective Review," *Progress in Energy and Combustion Science*, Vol. 17, 1991, pp. 327–371.

[2]Meltzer, J., Shepherd, J. E., Akbar, R., and Sabet, A., "Mach Reflection of Detonation Waves," *Dynamic Aspects of Detonations*, Vol. 153, Progress in Astronautics and Aeronautics, AIAA, Washington, DC, 1991, pp. 78–94.

[3]von Neumann, J., *Collected Works*, Vol. 6, Pergamon, New York, 1963, pp. 238–308.

[4]Gavrilenko, T. P., Nikolaev, Y. A., and Tpchiyan, M. R., "Supercompressed Detonation Waves," *Combustion, Explosion and Shock Waves*, Vol. 15, No. 5, 1980, pp. 659–692.

[5]Edwards, D. H., Walker, J. R., and Nettleton, M. A., "On the Propagation of Detonation Waves along Wedges," *Archival of Combustion*, Vol. 4, No. 3, 1984, pp. 197–209.

[6]Gavrilenko, T. P., and Prokhorov, E. S., "Compressed Detonation Wave in a Real Gas," *Combustion, Explosion and Shock Waves*, Vol. 17, No. 6, 1982, pp. 689–692.

[7]Gavrilenko, T. P., and Prokhorov, E. S., "Overdriven Gaseous Detonations," *Shock Waves, Explosions and Detonations*, Vol. 87, Progress in Astronautics and Aeronautics, AIAA, New York, 1983, pp. 244–250.

[8]Yu, Q., and Grönig, H., "Numerical Simulation on the Reflection of Detonation Waves," *Shock Waves*, edited by B. Sturtevant, J. E. Shepherd, and H. G. Hornung, Vol. 2, World Scientific, 1995, pp. 1143–1148.

[9]Liu, J. C., Liou, J. J., Sichel, M., Kauffman, C. W., and Nicholls, J. A., "Diffraction and Transmission of a Detonation into a Bounding Explosive Layer," *Twenty-First Symposium (International) on Combustion*, Combustion Inst., Pittsburgh, PA, 1986, pp. 1639–1647.

[10]Li, C., Kailasanath, K., and Oran, E. S., "Detonation Structures Behind Oblique Shocks," *Physics of Fluids*, Vol. 6, No. 4, 1994, pp. 1600–1611.

[11]Lee, J. H. S., "Dynamic Parameters of Gaseous Detonations," *Annual Review of Fluid Mechanics*, Vol. 16, 1984, pp. 311–336.

[12]Bartlmä, F., "The Propagation of Detonation Waves in Channels of Varying Cross-Section," *Journal of Fluid Mechanics*, Vol. 218, 1990, pp. 225–238.

[13]Fickett, W., and Davis, W. C., *Detonation*, Univ. of California Press, Berkeley, CA, 1979.

[14]Fickett, W., *Introduction to Detonation Theory*, Univ. of California Press, Berkeley, CA, 1985.

[15]Kailasanath, K., Oran, E. S., Boris, J. P., and Young, T. R., "Determination of Detonation Cell Size and the Role of Transverse Waves in Two-Dimensional Detonations," *Combustion and Flame*, Vol. 61, 1985, pp. 199–209.

[16]DeVore, C. R., and Oran, E. S., "The Stability of Imploding Detonations in the Geometrical Shock Dynamics (CCW) Model," *Physics of Fluids A*, No. 4, 1992, pp. 835–844.

[17]Ben-Dor, G., *Shock Wave Reflection Phenomena*, Springer–Verlag, New York, 1991.

[18]Emanuel, G., *Gasdynamics: Theory and Applications*, AIAA Education Series, AIAA, New York, 1986.

[19]Gordon, S., and McBride, B., NASA Rept. SP-273, 1971.

K. Kailasanath
Associate Editor